Hindawi
Mathematical Problems in Engineering
Volume 2023, Article ID 9847358, 1 page
https://doi.org/10.1155/2023/9847358

Retraction

Retracted: Application of Addition and Multiplication Noise Model Parameter Estimation in INSAR Image Processing

Mathematical Problems in Engineering

Received 13 September 2023; Accepted 13 September 2023; Published 14 September 2023

This article has been retracted by Hindawi following an investigation undertaken by the publisher [1]. This investigation has uncovered evidence of one or more of the following indicators of systematic manipulation of the publication process:

(1) Discrepancies in scope
(2) Discrepancies in the description of the research reported
(3) Discrepancies between the availability of data and the research described
(4) Inappropriate citations
(5) Incoherent, meaningless and/or irrelevant content included in the article
(6) Peer-review manipulation

The presence of these indicators undermines our confidence in the integrity of the article's content and we cannot, therefore, vouch for its reliability. Please note that this notice is intended solely to alert readers that the content of this article is unreliable. We have not investigated whether authors were aware of or involved in the systematic manipulation of the publication process.

Wiley and Hindawi regrets that the usual quality checks did not identify these issues before publication and have since put additional measures in place to safeguard research integrity.

We wish to credit our own Research Integrity and Research Publishing teams and anonymous and named external researchers and research integrity experts for contributing to this investigation.

The corresponding author, as the representative of all authors, has been given the opportunity to register their agreement or disagreement to this retraction. We have kept a record of any response received.

References

[1] G. Cui, "Application of Addition and Multiplication Noise Model Parameter Estimation in INSAR Image Processing," *Mathematical Problems in Engineering*, vol. 2022, Article ID 3164513, 10 pages, 2022.

Hindawi
Mathematical Problems in Engineering
Volume 2022, Article ID 3164513, 10 pages
https://doi.org/10.1155/2022/3164513

Research Article

Application of Addition and Multiplication Noise Model Parameter Estimation in INSAR Image Processing

Ge Cui

College of Educational Science and Technology, Anshan Normal University, Liaoning 114007, China

Correspondence should be addressed to Ge Cui; cuige@mail.asnc.edu.cn

Received 11 April 2022; Revised 24 April 2022; Accepted 28 April 2022; Published 19 May 2022

Academic Editor: Zaoli Yang

INSAR images are inevitably contaminated by noise during the process of generation, transmission, compression, and reception. Noise not only affects the quality of the INSAR image, but also affects subsequent operations such as the design of corresponding filters, INSAR image segmentation, compression, restoration, and feature recognition. The INSAR image noise model is mainly divided into additive noise and multiplicative noise. Compared with additive noise, multiplicative noise is more complicated due to INSAR image correlation and non-Gaussian. Based on least squares algorithm system of additive and multiplicative mixed noise model, this paper proposes a method of using PCA to remove multiplicative gamma distribution noise. The pure noise coefficient is obtained by subtracting the original coefficient from the diagonal wavelet coefficient of the noisy image, and the mode of the local variance is calculated as the estimation value of the noise standard deviation. Experiments show that the proposed method can obtain more accurate estimation of noise; in particular in the case of less noise and more detailed image information, its effect is more obvious.

1. Introduction

INSAR images can describe objective objects as intuitively and vividly as possible, and they have become an indispensable information carrier in our lives. The relevant information of the described object can be well displayed by the INSAR image, and people can receive the INSAR image through vision and obtain the information. And with the increase in the types of communication tools and various digital products and the large number of popularization and application, the use of INSAR images to convey information has gradually penetrated all aspects of life. The emergence of digital INSAR image processing technology makes it more realistic to use INSAR images to convey information, and its scope of use has become wider. However, in the following process of INSAR image formation, collection, transmission, reception, etc., it is inevitably affected by other factors, which interfere with the quality of the INSAR image and are called noise [1, 2]. Image noise classification standards are diverse, such as according to noise source classification, according to the shape of the spectrum, and according to the impact of noise on the image.

Noise greatly affects the structure and texture of the original INSAR image, resulting in reduced INSAR image quality and poor visual perception, and it becomes the biggest obstacle to some subsequent operations, such as target detection, INSAR image feature extraction, and parameter measurement and so on, which are inevitably affected by noise [3, 4]. Not only that, but there are many algorithms that need to know the prior knowledge of INSAR image noise in advance to a certain extent; otherwise it is not easy to expand, such as INSAR image noise reduction and INSAR image restoration [5, 6]. Because noise has the character of random variable, noise intensity is usually measured by variance in probability statistics. The INSAR image processing is shown in Figure 1.

In the past few decades, a variety of new methods and tools have been successfully applied to INSAR image

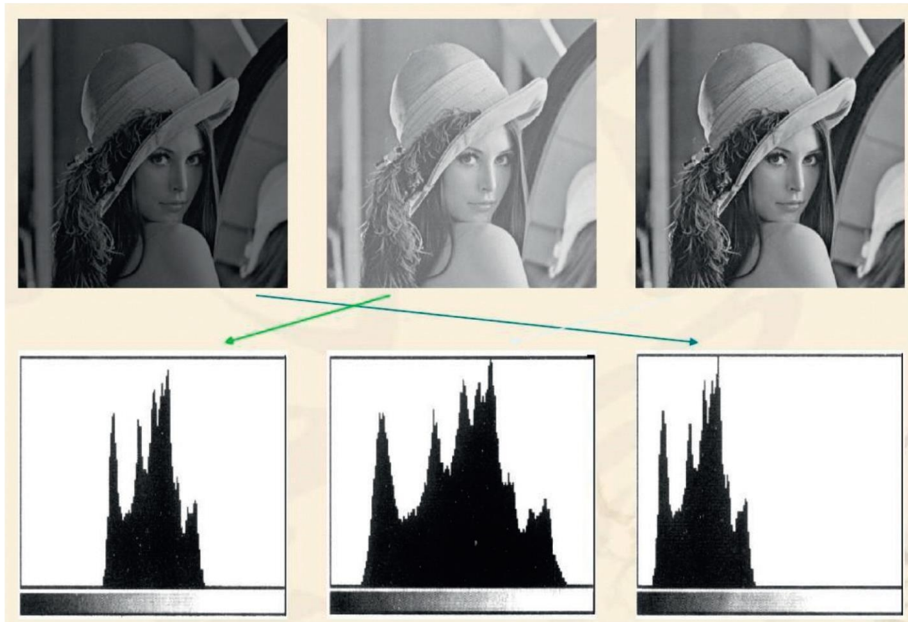

Figure 1: INSAR image processing.

processing, including random methods based on the Markov random field in probability statistics and Bayesian analysis principles, with wavelet-centered harmonics [7, 8], wave analysis methods, linear or nonlinear partial differential equation methods, and variational methods, etc. [9, 10]. In the study of noise parameter estimation, the following kinds of estimation methods are preliminarily formed, which are estimated by filtering method.

The most common denoising algorithm based on probability and statistics is the method using Markov Random Fields (MRF) [11, 12]. Usually it has two processing methods: one is to use the potential function to establish a probability distribution model on the basis of statistical signal processing and to obtain the solution through the maximum posterior probability estimation; the other is to use the potential of the MRF model in the method based on regularization. The function forms a priori constraints, and the solution is obtained through optimization [13, 14].

The method based on wavelet analysis is based on statistical signal processing, using general prior knowledge, selecting the appropriate filter, and learning and training to obtain the best estimation result for the test sample data set of the specific problem [15, 16]. As wavelet has made more and more outstanding achievements in signal processing and other fields and has received more and more attention, the literature introduces the theory and algorithm of wavelet in detail [17, 18]. As a powerful and effective processing tool for nonstationary signals and INSAR image signals, wavelet has been introduced into the application of SAR INSAR image speckle noise suppression, and more and more wavelet-based speckle suppression algorithms have emerged. The wavelet-based ripple suppression algorithm transforms the SAR INSAR image into the wavelet domain through wavelet transform and processes the wavelet coefficients in the wavelet domain [19, 20]. The processed wavelet coefficients are then subjected to wavelet inverse transformation to obtain a denoised filtered INSAR image. The soft and hard threshold method based on wavelet transform proposed by Donoho uses a threshold to compress the interfered wavelet transform coefficients. After the threshold, the noise is suppressed to a certain extent, and the edge information of the INSAR image is almost rarely lost. Someone analyzed the statistical distribution of speckle noise after wavelet decomposition and then combined the statistical characteristics of speckle noise in the wavelet domain to determine the soft threshold to achieve a better filtering effect. In order to make better use of wavelet transform to suppress SAR INSAR image speckle noise, it is very important to consider the statistical properties of wavelet coefficients after two-dimensional wavelet transform of SAR INSAR images and their correlation properties. Therefore, seeking a model that can fully reflect the correlation statistical characteristics between wavelet coefficients has become the key to wavelet denoising technology [21, 22]. In addition, some people use the characteristics of transform domain for estimation, as well as the segmentation method and the latest method of studying noise estimation based on statistical analysis.

The method based on the partial differential diffusion equation is to directly establish the partial differential equation, that is, the diffusion equation, for the problem to be solved. At the same time, a certain solution condition is added, and the established equation is solved by the optimized method to obtain the solution of the problem [23, 24]. This type of method directly establishes the diffusion equation based on the INSAR image information and diffuses the INSAR image to achieve the purpose of denoising. Perona and Malik proposed the well-known anisotropic diffusion model in 1990, which provided a new research direction in the field of INSAR image processing. The principle of this method of denoising is as follows: the smoothing process is carried out along the edge of the INSAR image, and filtering is suppressed in the direction of the vertical edge, thereby eliminating noise. The partial differential equation form of isotropic diffusion can be modified to obtain the anisotropic diffusion equation such as Lee filter and Frost6 filter [25, 26]. In this way, the partial differential equation and the adaptive filter are combined to greatly improve the filtering performance [27, 28].

Generally speaking, noise estimation based on statistical analysis is the most widely used estimation algorithm at present. The current various denoising methods are mostly based on the spatial domain and transform domain of the INSAR image for processing. The spatial domain method is to directly process the gray value of each pixel in the two-dimensional space where the INSAR image is located. Common methods include mean filtering, median filtering, Wiener filtering, bilateral filtering, nonlocal average filtering, and so on. The basic idea of mean filtering is to replace the gray value of the pixel to be processed with the average of the gray levels of several pixels and achieve a smoothing effect by dispersing the gray level of the mutation point in its neighboring points. Its operation is simple. However, it may blur the INSAR image. The method based on variation is to establish an objective function for INSAR image restoration and incorporate appropriate prior constraints into the objective function. Therefore, it may help to use an optimization method to obtain the desired solution. Variation-based methods can be used to complete INSAR image denoising, deblurring, restoration, and super-resolution processing. The basic idea of this kind of method is to use appropriate regularization techniques to form a new objective function on the basis of variation, and to obtain the extreme value of the objective function, the desired solution can be obtained. The development and application of variational methods are becoming more and more extensive. In addition, partial differential models can be analyzed from a variational perspective. In recent years, for multiplicative noise, researchers have proposed models to eliminate the impact of multiplicative noise on INSAR image quality to a certain extent [29].

Later, researchers started from the aspects of how to choose the size, shape, and direction of the neighborhood, how to choose the number of points involved in the average, and how to determine the weight coefficient of each point in the neighborhood and successively proposed a variety of local-based smoothing algorithms. Median filtering is a nonlinear signal processing method, which replaces the value of a point in a digital INSAR image or digital sequence with the median value of each point in a neighborhood of the point. The median filter algorithm is less robust because of the size and shape of the window, and hence it will have a greater impact on the filtering effect and it is actually unpredictable. On the other hand, the median filter does not make full use of the statistical knowledge of the observed INSAR image information available in practice, and thus it is a nonparametric estimation. Wiener filtering adjusts the output of the filter according to the local variance of the INSAR image. It is an adaptive filtering method. Scholars such as Buades proposed the NonLocalMeans Algorithm, which greatly improves the quality of INSAR image denoising. Nonlocal average filtering makes full use of the redundant information in the natural INSAR image. Its main feature is to compare all the gray distributions in the windows surrounding the processed pixels and to contribute weights based on the similarity of the gray distributions. The processed gray value of the processed pixel is the weighted average sum of all similar points. The noise estimation based on statistical analysis can achieve better denoising effect and reduce the complexity of the algorithm.

Transform domain filtering is to transform the original spatial INSAR image into the frequency domain for processing by passing the pixel value INSAR image in the natural space through a certain transformation. After processing, it is converted back to the spatial domain through inverse transformation to restore the INSAR image to achieve the purpose of denoising. The transformed frequency domain coefficients are obviously distributed. Many signals that cannot be effectively analyzed in the spatial domain can be effectively analyzed when placed in the frequency domain, which is beneficial to various INSAR image processing tasks. There are many ways to transform an INSAR image from the spatial domain to the transform domain, such as Fourier Transform, Discrete Cosine Transform, Wavelet Transform, Multiscale Geometric Analysis, etc. The traditional algorithms of frequency domain denoising include low-pass filtering, high-pass filtering, soft and hard threshold filtering, etc. Through the spectrum analysis of the INSAR image, we know that the INSAR image detail component and the noise have the same spectrum component as the high-frequency component. According to the first the experimental INSAR image information processes the signal in the transform domain to eliminate noise.

At present, the research of various denoising methods is carried out under the condition of subjective inference or assuming that the noise is of a known type and known parameters, but the prior knowledge of noise is unknown in practical applications. In turn, the blindness of INSAR image noise processing is increased, and the effect of noise removal is unsatisfactory. Although the current denoising methods are diverse and cover a wide range, it is precisely because of the unknown prior knowledge of noise that various denoising methods have their own strengths, and their effects on different types and sizes of noise are very different. Studies have shown that even the best noise removal method cannot be suitable for all types of noise. Thus, based on least squares algorithm system of additive and multiplicative mixed noise model, this paper proposes a method of using PCA to remove multiplicative gamma distribution noise.

2. Noise Model

Noise is an important cause of image interference. During INSAR image formation, transmission, reception, processing, and subsequent applications, various links may produce noise interference, such as electronic component noise, camera tube noise, optical noise, machine noise, etc. These noises pass through various electronic circuits and equipment. Various deformations will occur, resulting in new types of noise, for example, according to the noise source, according to the cause of generation, according to the shape of the spectrum, and according to the effect of the noise on the INSAR image to classify the noise. Not only may the noise and the signal be correlated or statistically independent, but the noise itself may also be correlated or uncorrelated. Different noises in the INSAR image reflect different statistical characteristics. Therefore, there are many types of INSAR image noise, and considering different starting points, its classification standards are also diverse. The following chart is shown in Figure 2.

$$g(x, y) = f(x, y) + n(x, y),$$
$$g(x, y) = f(x, y) + f(x, y) \times n(x, y). \tag{1}$$

Among them, f is the true signal, the noise is n, and the observed signal is g.

2.1. Gaussian Noise. The MATLAB implementation of Gaussian noise is also relatively simple; one is to directly load the MATLAB toolbox.

With the built-in Gaussian noise in, the second is to use the randn(M, N) function to generate a Gaussian noise matrix with mean a, variance b, and size MN pixels, as follows:

$$z = a + b. * \mathrm{rand}\, n(M, N), \tag{2}$$

where a is the mean value of Gaussian noise to be added, b is the variance, and M and N are the size of the gray INSAR image to be noised.

2.2. Uniform Noise. Uniform noise obeys uniform distribution. Assuming that the uniform distribution interval is [a, b], in the process of generating INSAR image noise, we cannot distinguish the possibility of random noise z taking different values in the interval [a, b]. It can be assumed that z obeys a uniform distribution on [a, b]. Uniform noise can also be directly generated by rand$n$(M, N) and then loaded into the original grayscale INSAR image. The uniform noise matrix is as follows:

$$z = a + (b - a) * \mathrm{rand}(0, 1), \tag{3}$$

where z is the added noise matrix, and a and b are the distribution interval parameters of uniform noise. In this case, the uniform noise matrix can also be directly generated by rand(M, N).

2.3. Salt and Pepper Noise. The wavelet transform used in the INSAR image is generally a two-dimensional separable wavelet transform. When processing the INSAR image, two one-dimensional transforms are required; that is, the rows are first transformed, and then the transformed rows are transformed by columns. Salt and pepper noise is also called double impulse noise. INSAR image sensors, transmission channels, decoding processing, etc. will cause salt and pepper noise in the INSAR image. Generally, pepper noise and salt noise appear at the same time and appear as black and white dot noise. The realization of salt and pepper noise requires some logical judgment. We consider generating uniform noise first, and then by setting the threshold, the points outside the threshold are set as black points or white points to realize the simulation of salt and pepper noise. Of course, you can also directly load the salt and pepper noise that comes with MATLAB.

2.4. Rayleigh Noise. The wavelet transform used in the INSAR image is generally a two-dimensional separable wavelet transform. When processing the INSAR image, two one-dimensional transforms are required; that is, the rows are first transformed, and then the transformed rows are transformed by columns. When there is a random two-dimensional vector, and its two components are independent of each other and obey the normal distribution with the same variance, the modulus of this vector obeys the Rayleigh distribution. The realization of Rayleigh noise can be done by averaging the noise, as follows:

$$z = a + \sqrt{-b \ln[1 - U(0, 1)]}. \tag{4}$$

Here $U(0, 1)$ means uniform distribution, the parameters of uniform distribution are as follows: the mean is 0, and the variance is 1. In MATLAB, the use of the function rand(M, N) can easily generate uniform noise, and the mean is 0 and the variance is 1. The INSAR image with/without noise is shown in Figure 3.

2.5. Gamma Noise. The noise whose amplitude obeys the density distribution function of the gamma curve is gamma noise. How gamma noise is generated by MATLAB: its realization can be superimposed by b noises that obey the exponential distribution.

$$E_i = -\frac{1}{a}\ln[(1 - U(0, 1))],$$
$$z = E_1 + E_2 + \cdots + E_b, \tag{5}$$

where E_i is an exponential random sequence with parameter a, z is the gamma noise matrix generated by the superposition of E_b, and b is a constant.

2.6. Exponential Noise. Exponential distribution is a special case of gamma distribution. Exponentially distributed noise can be realized by a random matrix generated by rand(M, N).

$$E = -\frac{1}{a}\ln[1 - \mathrm{random}(0, 1)], \tag{6}$$

where a is a constant. The probability density function curve of common noise is shown in Figure 4.

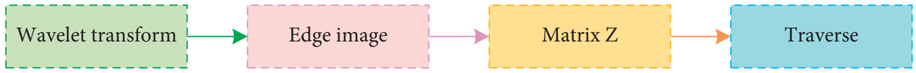

Figure 2: Following chart.

Figure 3: INSAR image with or without noise.

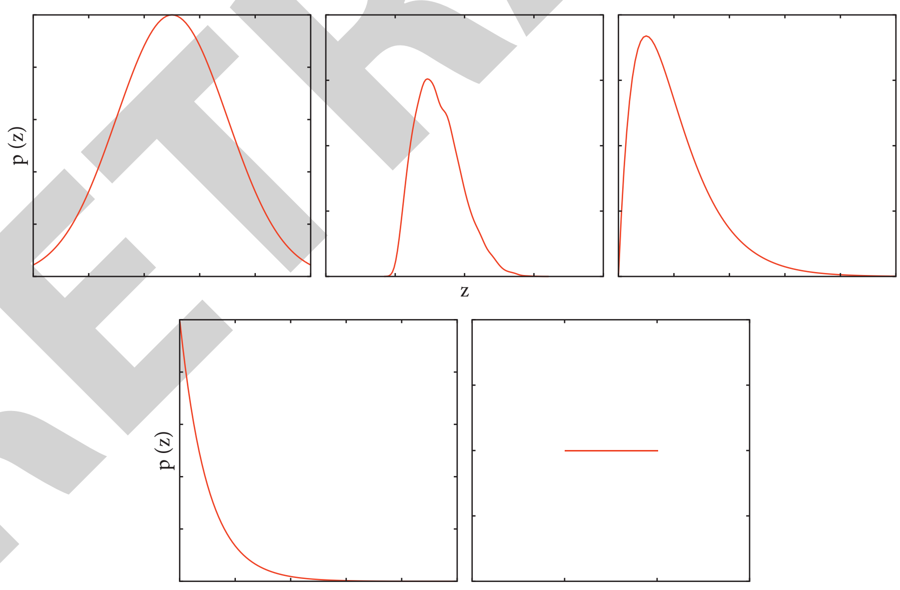

Figure 4: Probability density function curve of common noise.

3. Estimation of Noise Model Parameters

Because there are many types of wavelet function $\Psi(x)$ in wavelet transform, and the characteristics of each wavelet function are different, there are commonalities and differences. For different purposes, the choice of wavelet base should be different, so as to achieve a better decomposition or reconstruction effect. Therefore, it is necessary to choose a suitable wavelet function according to the different purposes used. The power analysis is shown in Figure 5. The variance of noise is estimated by using statistical method for the coefficients of diagonal wavelet of noisy images, but the

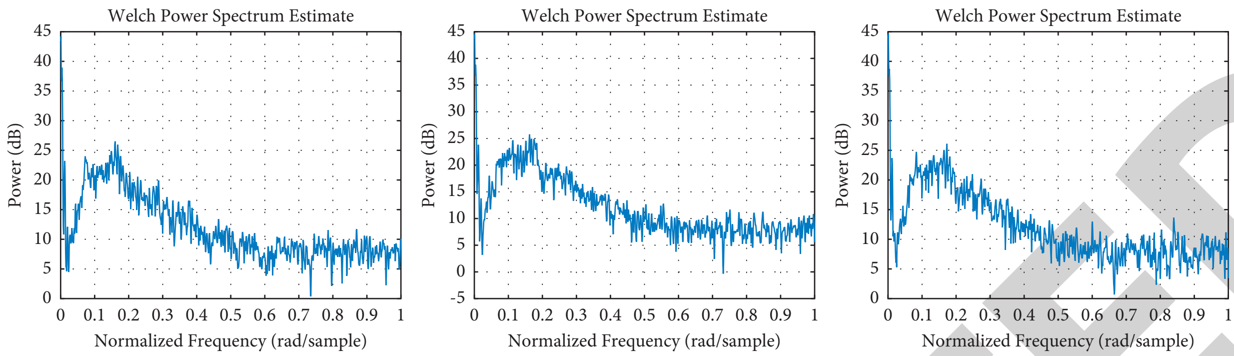

Figure 5: Power analysis.

premise is that the coefficients of diagonal wavelet are basically noise signals.

The wavelet transform used in the INSAR image is generally a two-dimensional separable wavelet transform. When processing the INSAR image, two one-dimensional transforms are required; that is, the rows are first transformed, and then the transformed rows are transformed by columns. Different wavelet basis functions have different characteristics, and application objects have their own requirements, so consider the principles of wavelet basis and the requirements of application objects. The general principles of wavelet basis function are the length of wavelet support, the order of vanishing distance, regularity, and symmetry. 1. Orthogonality: Because it simplifies the difficulty of mathematical analysis, it is easier to operate in engineering applications. 2. Compact support: Its characteristic is that the realization of the algorithm is relatively easy, because it can exert the advantages of time-frequency local characteristics. 3. Symmetry: This characteristic affects the distortion problem. Consider whether it has linear phase filtering characteristics. 4. Smoothness: This is a characteristic related to resolution.

Of course, it is impossible for a wavelet basis function to be perfect enough to fully satisfy these characteristics at the same time. For example, it is impossible to satisfy both compact support and smoothness at the same time. Similarly, compact support and smoothness have an impact on the symmetry of the wavelet function. Only in the case of comprehensive consideration and comprehensive analysis, a compromise solution can be selected. Because the next step is to analyze the noise of the INSAR image, the selected wavelet base can highlight the components to be processed, and there are similarities between the two. In actual operation, because the db1 wavelet is an orthogonal wavelet that not only has symmetry but also satisfies tight support, and because its unitary transformation characteristic can ensure that the statistical characteristics of noise are not changed, we choose the db1 wavelet basis for wavelet decomposition.

The generalized Gaussian distribution characteristics of wavelet coefficients will be affected by the complexity of the INSAR image texture and structure, and the richer the texture, the more obvious the generalized Gaussian distribution characteristics. But how to filter out the INSAR image texture part that meets the requirements and use it in noise estimation is still more difficult to solve. Wavelet transform has the following characteristics. It can suppress a part of the texture information of the original INSAR image, and at the same time, it can better ensure that the noise part is less affected. Specifically, the multiresolution feature of wavelet transform makes it easy to extract the high-frequency components of the INSAR image. Use wavelet transform to decompose the noisy INSAR image. After decomposition, most of the information that can represent the important characteristics of the INSAR image is concentrated on a few large wavelet coefficients, while most of the INSAR image noise and a small amount of original INSAR image information are generally reflected on high-frequency detail coefficients with small amplitudes. That is, noise information and a very small part of the original INSAR image information are concentrated in the high-frequency part, and the INSAR image information is concentrated in the low-frequency part. However, although both the horizontal detail subband cH and the vertical detail subband cV belong to the high-frequency detail subband, they are easily affected by the directional edges of the INSAR image, which makes them inappropriate to represent the high-frequency details of the INSAR image. At the same time, the detailed corner subband cD is less affected by the directional structure of the INSAR image but can reflect the overall details of the INSAR image, so the diagonal detail subband can be used to express the high-frequency details of the INSAR image. The time analysis based on MATLAB is shown in Figure 6.

In previous studies, a theory of "INSAR image local consistency" was proposed, which refers to uncontaminated natural INSAR images; their local variance distribution will achieve the maximum probability at a value of 0. Based on the above theory, the literature verifies and draws a conclusion: the majority of local variance values are distributed around 0, and the probability distribution curve starts to decrease exponentially from 0. Analyzing the above conclusions, in principle, the local area of the natural INSAR image should have relatively low variability. In other words, the local variance of the original INSAR image should be characterized by high peaks, which can be expressed by the mode. The local variance value with the highest probability of occurrence should be close to zero. Therefore, when the noise variance is estimated for a noisy INSAR image, the mode of the INSAR image local variance can be used as an

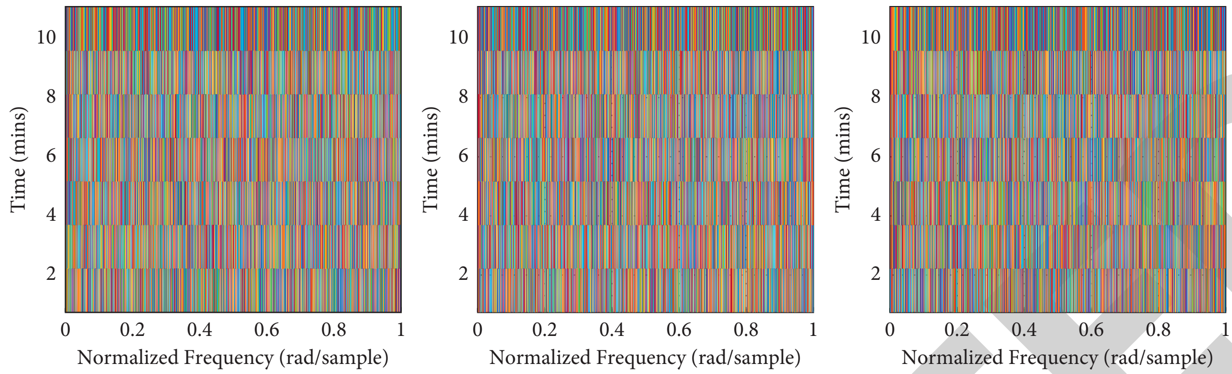

Figure 6: Time analysis.

effective estimator. Because the local variance distribution of the noise INSAR image is equivalent to the right shift of the local variance distribution of the original INSAR image, the magnitude of its movement can be used to approximate the noise variance.

However, according to the literature, the INSAR image composition is complicated or contains a lot of texture structure, which will lead to the failure of the hypothesis of INSAR image. In this way, if you continue to use the mode of the distribution of the local variance of the noisy INSAR image to estimate the size of the noise, it will no longer be accurate. How to maintain the assumption of "local INSAR image consistency" and make it less affected by the texture structure becomes more important. Through the foregoing "local hypothesis consistency" being affected by the texture structure of the INSAR image, and the unitary invariance of the statistical characteristics of the noise in the transform domain, the extraction of the wavelet coefficients of the diagonal subbands of the noisy INSAR image can not only suppress a part of the texture information of the original INSAR image, but also better retain noise information. Therefore, using the mode of the local variance distribution of the high-frequency wavelet components of the noise INSAR image to estimate the variance of the noise is better than using the original INSAR image. The predicted value based on MATLAB is shown in Figure 7.

The wavelet transform used in the INSAR image is generally a two-dimensional separable wavelet transform. When processing the INSAR image, two one-dimensional transforms are required; that is, the rows are first transformed, and then the transformed rows are transformed by columns. The filter is used to describe the process as follows: the signal is decomposed into approximate coefficients (larger scale) and detail coefficients (smaller scale) through one-dimensional wavelet transform, which needs to pass through low-frequency and high-frequency filters; two-dimensional wavelet transform must be correct. Low-frequency filtering and high-frequency filtering are used for rows, and the same is true for columns. After transformation, the wavelet decomposition coefficients at the j-th layer are set as

$$\left[cA_j, cH_j, cV_j, cD_j\right]. \tag{7}$$

Analyze the filtering process in detail; the row and column dimensions are applied to the low-pass filter to get the approximate coefficients of the j-th layer; the horizontal and vertical are applied to the low-pass filter and the high-pass filter, respectively, and then the level components of the detail parameters, in turn, the horizontal. The vertical component is the vertical component after acting on the high-pass filter and the low-pass filter, respectively, and it is also a detail parameter. After the high-frequency filter is acted on both horizontally and vertically, it is the diagonal component, which is also the detail parameter. Let the INSAR image in the real domain be f, and use cDj to denote the high-frequency diagonal detail subband on the j-th scale after wavelet decomposition.

$$cD_j = f \times L_{j-1}^{D}, \tag{8}$$

where $*$ means convolution; after filtering operation,

$$L_{j-1}^{D} = H_0 * H_0' * \cdots H_{j-2} * H_{j-2}' * G_{j-1} * G_{j-1}'. \tag{9}$$

Then the norm of the filter is

$$\left\| L_{j-1} \right\| = \sqrt{\sum_{m} \sum_{m} L_{i-1}^{2}(m, n)}. \tag{10}$$

The noise estimation algorithm flowchart is shown in Figure 8.

(1) The wavelet decomposition coefficients of the INSAR image are obtained by filtering and sampling, and the multiscale decomposition is performed by iteration. The size of the 4 components obtained by the decomposition of each layer is 1/4 of the parent wavelet subband INSAR image of the upper layer; that is, the rows and columns of the next wavelet subband INSAR image between adjacent scales are 1/2 of the parent wavelet INSAR image of the previous scale. Since the algorithm in this paper is based on the correlation between adjacent scale subbands, it is necessary to treat the coefficient matrices of different scales as the same size. The filter used at this time needs to be adjusted. If the conventionally used filter is L_0, you need to insert 0 between each adjacent coefficient in L_0. Use the filter to insert 0 to achieve

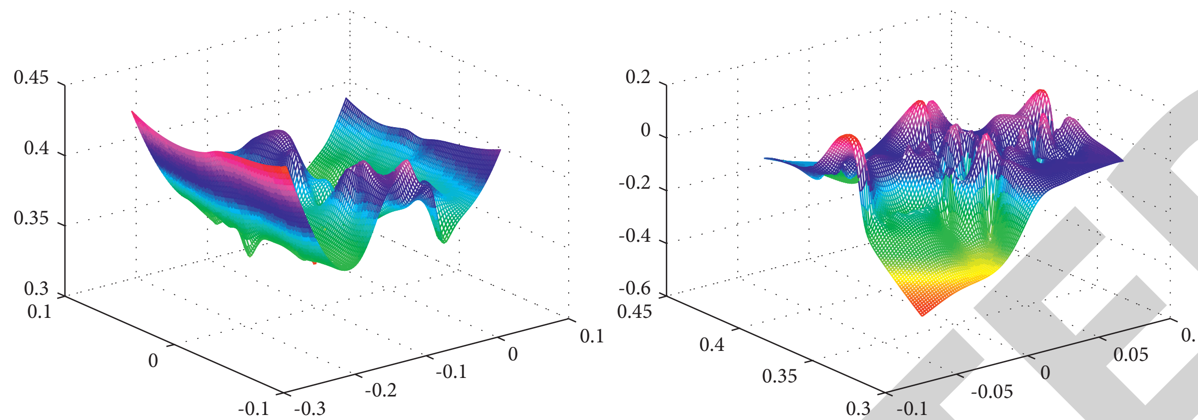

Figure 7: Predicted value.

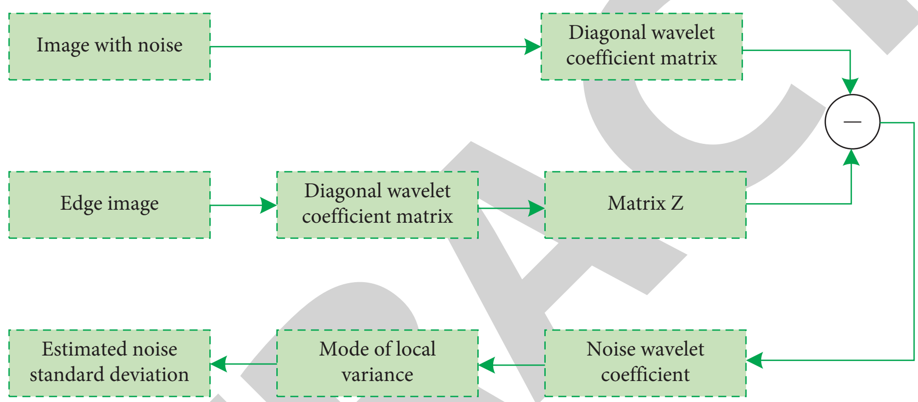

Figure 8: Noise estimation algorithm flowchart.

the reduction of the scale band, no longer through the way of downsampling.

(2) After verification, it is best not to estimate all the coefficients, because this will cause a large deviation. The analysis found that most of the information in the high-frequency subband itself can be considered as noise, and only a few coefficients with larger amplitudes are contributed by the original INSAR image. Estimation of coefficients with smaller amplitudes is basically composed of noise but will make the error larger. Because of this, in order to estimate only the coefficients with larger amplitudes, this algorithm uses the canny operator in the spatial domain to obtain the edge of the noisy INSAR image and then performs wavelet transformation on the obtained edge INSAR image to obtain the corresponding coefficient matrix. According to the obtained matrix, it is judged which part of the coefficients in the diagonal subband remains unchanged and which part of the coefficients is used as the estimated value. Considering that the wavelet transform itself has the effect of whitening, it will make the correlation of the transformed INSAR image coefficients worse, so the canny operator is not used in the transform domain, but first in the spatial domain and then the wavelet transform. The noise is optimized in Figure 9.

(3) Because the filter interpolation 0 is used to achieve the scale band reduction, this process requires two registrations of the wavelet coefficient matrix, one is the registration of the diagonal wavelet subband cD_1 and the adjacent scale subband cD_2, and the other one time is the cD_1 subband of the noisy INSAR image and the estimate is extracted. The basis of registration is to adopt the minimum mean square error criterion.

The specific algorithm steps are as follows:

(1) Perform wavelet transformation on the noisy INSAR image, let cD1 be the high-frequency diagonal subband and cD_2 be the subwavelet coefficients corresponding to the adjacent scales, match the two for use, and use the formula to get a rough estimate of the noise variance in the cD_1 subband.

(2) Perform edge extraction on the noisy INSAR image in the spatial domain to obtain the edge INSAR image. The operator used is canny, and then after wavelet transformation, cD_0 is defined as the resulting high-frequency diagonal subband.

Figure 9: Noise optimization of INSAR image.

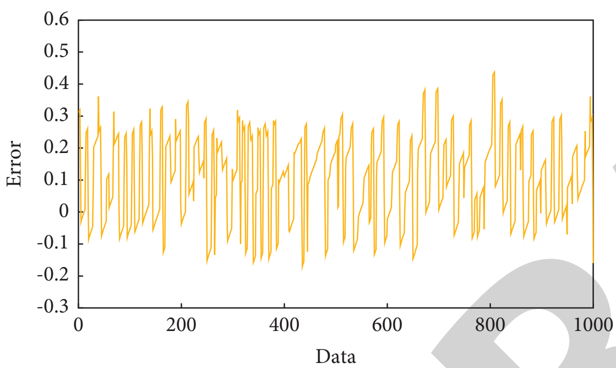

Figure 10: Precision.

(3) Generate a 0 matrix Z with the same size as cD_1 to represent the information of the original INSAR image in the diagonal subband.

(4) The matrix cD_0 is a transform domain matrix containing only the edge texture part of the INSAR image. The coefficients that are not 0 in it are traversed. At the same time, the coefficients in the same position in cD_1 may be retained or estimated according to the above mentioned algorithm. And import the estimated value into the 0 matrix Z. At this time, the matrix Z is the estimated value of the pure INSAR image in cD_1. The precision of the proposed method is shown in Figure 10.

4. Conclusion

Based on least squares algorithm system of additive and multiplicative mixed noise model, this paper proposes a method of using PCA to remove multiplicative gamma distribution noise. The specific methods are as follows:

(1) First, according to the characteristics of multiplicative noise, use logarithmic transformation to transform the original INSAR image from spatial domain to logarithmic domain, and convert multiplicative noise into additive noise.

(2) Secondly, constructed by selecting local similar blocks in the logarithmic domain in the training sample set, the principal component analysis method is used to extract the main features of the signal.

(3) In the transformation domain of principal component analysis, based on the linear minimum mean square error estimation, a threshold principle is given, and the noise is eliminated through the threshold.

(4) For the deviation caused by the number transformation, the INSAR image information in the logarithmic domain is exponentially transformed back to the spatial domain through bias estimation and correction to obtain a filtered INSAR image. The simulation results show that the algorithm in this paper can effectively remove the noise while retaining the details of the INSAR image.

Data Availability

The data used to support the findings of this study are available from the corresponding author upon request.

Conflicts of Interest

The author declares that are no known competing financial interests or personal relationships that could have appeared to influence the work reported in this paper.

Acknowledgments

This work was supported by Key Research Project of Anshan Normal University: Research on strategies for improving information literacy of preschool education students (no. 17kyxm18); Humanities and Social Science research project of Liaoning Education Department: Practical research on improving the core literacy of preschool education major students by relying on intelligent teaching mode (no. 20190609).

References

[1] Y. Yu, C. Yang, Q. Deng, T. Nyima, S. Liang, and C. Zhou, "Memristive network-based genetic algorithm and its application to INSAR image edge detection," *Journal of Systems Engineering and Electronics*, vol. 32, no. 5, pp. 1–9, 2021.

[2] Y. Ishida and S. Hashimoto, "Asymmetric characterization of diversity in symmetric stable marriage problems: an example of agent evacuation," *Procedia Computer Science*, vol. 60, no. 1, pp. 1472–1481, 2015.

[3] P. Zoha and R. Kaushik, "INSAR image edge detection based on swarm intelligence using memristive networks," *IEEE Trans. on CAD of Integrated Circuits and Systems*, vol. 37, no. 9, pp. 1774–1787, 2018.

[4] J. Pais, "Random matching in the college admissions problem," *Economic Theory*, vol. 35, no. 1, pp. 99–116, 2008.

[5] J. J. Jung and G. S. Jo, "Brokerage between buyer and seller agents using constraint satisfaction problem models," *Decision Support Systems*, vol. 28, no. 4, pp. 291–384, 2020.

[6] Y. Liu and K. W. Li, "A two-sided matching decision method for supply and demand of technological knowledge," *Journal of Knowledge Management*, vol. 21, no. 3, pp. 592–606, 2017.

[7] J. Byun and S. Jang, "Effective destination advertising: matching effect between advertising language and destination type," *Tourism Management*, vol. 50, no. 10, pp. 31–40, 2015.

[8] A. N. Nagamani, S. N. Anuktha, N. Nanditha, and V. K. Agrawal, "A genetic algorithm-based heuristic method for test set generation in reversible circuits," *IEEE Transactions on Computer-Aided Design of Integrated Circuits and Systems*, vol. 37, no. 2, pp. 324–336, 2018.

[9] C. Koch and S. P. Penczynski, "The winner's curse: conditional reasoning and belief formation," *Journal of Economic Theory*, vol. 174, pp. 57–102, 2018.

[10] C. K. Karl, "Investigating the winner's curse based on decision making in an auction environment," *Simulation & Gaming*, vol. 47, no. 3, pp. 324–345, 2016.

[11] D. Ettinger and F. Michelucci, "Creating a winner's curse via jump bids," *Review of Economic Design*, vol. 20, no. 3, pp. 173–186, 2016.

[12] J. A. Brander and E. J. Egan, "The winner's curse in acquisitions of privately-held firms," *The Quarterly Review of Economics and Finance*, vol. 65, pp. 249–262, 2017.

[13] Z. Palmowski, "A note on var for the winner's curse," *Ekonomia XXI Wieku*, vol. 3, no. 15, pp. 124–134, 2017.

[14] B. R. Routledge and E. Z. Stanley, "Model uncertainty and liquidity," *Review of Economic Dynamics*, vol. 12, no. 4, pp. 543–566, 2009.

[15] D. Easley and M. O'Hara, "Ambiguity and nonparticipation: the role of regulation," *Review of Financial Studies*, vol. 22, no. 5, pp. 1817–1843, 2009.

[16] P. Klibano, M. Marinacci, and S. Mukerji, "A smooth model of decision making under ambiguity," *Econometrica*, vol. 73, no. 6, pp. 1849–1892, 2005.

[17] Y. Halevy, "Ellsberg revisited: an experimental study," *Econometrica*, vol. 75, no. 2, pp. 503–536, 2007.

[18] D. Ahn, S. Choi, D. Gale, and K. Shachar, "Estimating ambiguity aversion in a portfolio choice experiment," *Working paper*, vol. 5, no. 2, pp. 195–223, 2019.

[19] T. Hayashi and R. Wada, "Choice with imprecise information: an experimental approach," *Theory and Decision*, vol. 69, no. 3, pp. 355–373, 2010.

[20] K. Zima, E. Plebankiewicz, and D. Wieczorek, "A SWOT Analysis of the Use of BIM Technology in the Polish Construction Industry," *Buildings*, vol. 10, no. 1, 2020.

[21] P. Sun, B. Liu, and T. Sun, "Injury status and strategies of female 7-a-side rugby players in Anhui Province," *Sports Boutique*, vol. 38, no. 3, pp. 72–74, 2019.

[22] P. Guild, M. R. Lininger, and M. Warren, "The association between the single leg hop test and lower-extremity injuries in female athletes: a critically appraised topic," *Journal of Sport Rehabilitation*, vol. 30, no. 2, pp. 1–7, 2020.

[23] U. G. Inyang, E. E. Akpan, and O. C. Akinyokun, "A hybrid machine learning approach for flood risk assessment and classification," *International Journal of Computational Intelligence and Applications*, vol. 19, no. 2, Article ID 2050012, 2020.

[24] Q. Liu, S. Du, B. J. van Wyk, and Y. Sun, "Double-layer-clustering differential evolution multimodal optimization by speciation and self-adaptive strategies," *Information Sciences*, vol. 545, no. 1, pp. 465–486, 2021.

[25] H. R. Medeiros, F. D. de Oliveira, H. F. Bassani, and A. F. Araujo, "Dynamic topology and relevance learning SOM-based algorithm for image clustering tasks," *Computer Vision and Image Understanding*, vol. 179, pp. 19–30, 2019.

[26] Y. Deng, D. Huang, S. Du, G. Li, and C. Zhao, "A double-layer attention based adversarial network for partial transfer learning in machinery fault diagnosis," *Computers in Industry*, vol. 127, Article ID 103399, 2021.

[27] J. J. Chan, K. K. Chen, S. Sarker et al., "Epidemiology of Achilles tendon injuries in collegiate level athletes in the United States," *International Orthopaedics*, vol. 44, no. 3, pp. 585–594, 2020.

[28] W. Li, G. G. Wang, and A. H. Gandomi, "A survey of learning-based intelligent optimization algorithms," *Archives of Computational Methods in Engineering*, vol. 28, pp. 1–19, 2021.

[29] G. G. Wang, A. H. Gandomi, A. H. Alavi, and D Gong, "A comprehensive review of krill herd algorithm: variants, hybrids and applications," *Artificial Intelligence Review*, vol. 51, no. 1, pp. 119–148, 2019.